Determining the pulse-echo electromechanical characteristic of a transducer using flat-plates and point targets [a)]

Thomas L. Szabo [b)]
Department of Aerospace and Mechanical Engineering, Boston University, Boston MA 02115

Başak Ülker Karbeyaz [c)]
Department of Electrical Engineering and Computer Science, Northeastern University, Boston MA 02115

Robin O. Cleveland [d)]
Department of Aerospace and Mechanical Engineering, Boston University, Boston MA 02115

Eric L. Miller [e)]
Department of Electrical Engineering and Computer Science, Northeastern University, Boston MA 02115

Received:

Short title: Calibration using flat-plates and point scatterers

Running title: Calibration using flat-plates and point scatterers

[a)] Submitted in June 2003 to the Journal of the Acoustical Society of America.
[b)] Electronic mail: tlszabo@bu.edu
[c)] Electronic mail: bulker@ece.neu.edu
[d)] Electronic mail: robinc@bu.edu
[e)] Electronic mail: elmiller@ece.neu.edu

ABSTRACT

A common technique to determine the electromechanical response of a spherically focusing transducer is to use a reference pulse-echo from a flat-plate in the focal plane of the transducer. We show that when the pressure focusing gain of the transducer is much greater than unity, the focal plane reflection is a valid approximation of the desired electromechanical response. An alternative calibration target is a point scatterer and we show theoretically and experimentally that this waveform is the double time differential of the flat-plate response. The use of calibration to describe general scatterers through a Born approximation (Jensen, J. Acoust. Soc. Am. 89:182-190) is discussed.

PACS numbers: 43.20.Fn, 43.20.Rz, 43.20.Bi, 43.35.Bf

I. INTRODUCTION

In pulse-echo ultrasound imaging a single transducer is used to both transmit an acoustic pulse and receive acoustic echoes. An electromechanical transfer function is associated with the transducer for both the transmit process (converting the electrical excitation into an acoustic disturbance) and the receive process (converting the acoustic disturbance into an electrical signal). To characterize the emitted and received acoustic pulse and to accomplish transducer calibration, the electromechanical response of the transducer must be determined.

The common practice to calibrate a transducer is to place a large flat-plate either on the beam axis in the extreme nearfield or farfield of a nonfocusing transducer or in the focal plane of a focusing transducer (Carpenter and Stepanishen, 1984; Chen et al., 1997; Machado and Foster, 1998). A waveform measured under these conditions, can, in principle, be used to aid in the removal or compensation of transducer response and field effects on the measurement of tissue properties (Carpenter and Stepanishen, 1984; Chen et al., 1997; Machado and Foster, 1998; Thijssen, 2000).

In this paper we provide a framework for calibration which consistently integrates much of the previous literature in this area (Hunt et al., 1983; Carpenter and Stepanishen, 1984; Madsen et al., 1984; Jensen, 1991; Bridal et al., 1996; Chen et al.,1997). We examine in detail the case of a spherically focused transducer and prove that the electromechanical response can also be measured by the use of a point target as well as a plate reflector. We show both theoretically and experimentally that the scattered signal from a plate and point target are related by double differentiation in time. We present a simple physical model which results in accurate simulation of the

backscattered field from arbitrary shaped weak scatterers. In particular, we bring to attention to a possible misinterpretation of data taken from a flat-plate when applied to scattering from a point target. This clarification is of importance for the time domain scattering theory of Jensen (1991) which is based on the impulse response of a point scatterer.

II. THEORY and BACKGROUND

In this section we discuss the theory of scattering of sound and the relation between the electromechanical impulse response of a transducer and the measured back scattered signal from specific obstacles. We consider the case of the received signal for a monostatic pulse-echo configuration although it is straightforward to generalize our results to bi-static geometries.

Following the notation in Jensen (1991) a model for the scattering process that has a simple physical interpretation as well as a straightforward implementation can be summarized by the following equation:

$$v_o(t) = v_i(t) *_t e_T(t) *_t h_T(\vec{r}, t) *_t s(\vec{r}, t) *_t h_R(\vec{r}, t) *_t e_R(t) \tag{1}$$

where $v_i(t)$ is the excitation voltage, $e_T(t)$ is the electromechanical response that is the ratio of the derivative of the normal particle velocity with respect to time relative to the transmit voltage, $h_T(\vec{r}, t)$ is the transmit spatial impulse response, $h_R(\vec{r}, t)$ is the receive spatial impulse response of the transducer located at position vector $\vec{r}$, $s(\vec{r}, t)$ is a scattering term located at $\vec{r}$ which accounts for perturbations or inhomogeneities in the medium that give rise to the scattered signal, $v_0(t)$ is the output voltage from

the transducer, $e_R(t)$ is the receive voltage to force electromechanical response, and $*_t$ is convolution with respect to time.

We define the round-trip pulse-echo electromechanical impulse response of the transducer, $e_{pe}(t)$ as:

$$e_{pe}(t) = v_i(t) *_t e_T(t) *_t e_R(t) \tag{2}$$

For the case where $v_i(t)$ is a very short electrical impulse (e.g., less than about $1/10^{th}$ of the characteristic period of the transducer) e_{pe} will be proportional to $e_T *_t e_R$ which is the true electromechanical impulse response of the transducer. Equation (1) can now be written as

$$v_o(t) = e_{pe}(t) *_t h_T(\vec{r}, t) *_t s(\vec{r}, t) *_t h_R(\vec{r}, t) \tag{3}$$

where the remaining terms account for propagation and scattering. If one assumes that the absorption of the medium (e.g. de-ionized and de-gassed water in the low megahertz frequencies) is negligible then analytical expressions exist for h_T and h_R for a spherically focused transducer (Arditi et al., 1981; Hunt et al., 1983). The scattering term $s(\vec{r}, t)$ depends on the target.

In this paper we will discuss scattering from three different obstacles: a flat-plate, a point target and an arbitrary shaped weak scatterer. The first two cases will be presented for calibration and the third for imaging applications that require such calibration.

A. Scattering from a flat-plate

In this section, we discuss the conditions under which the focal plane reflection from a flat-plate is a valid approximation of the electromechanical impulse response.

When the flat-plate is an ideal acoustic mirror placed at a distance from the transmitter, z, perpendicular to the beam axis, the receiver can be considered as the mirror image of the transmitter. Hence in pulse-echo imaging of an acoustic mirror, the problem is the same as that of two identical transducers separated by a distance $2z$, as shown by Rhyne (1977) for a nonfocusing transducer, and by Chen et al. (1994) for both nonfocusing and focusing transducers.

Rhyne (1977) derived a time domain expression for the reflection from a flat-plate and called it the "radiation coupling" function. This result is the same as the problem of finding diffraction loss, D_F, between two identical transducers at a distance $2z$ (Seki et al., 1958; Rogers and van Buren, 1974). In both cases, this loss represents the reduction in amplitude and change in phase when only a portion of a transmitted beam is intercepted by a receiving transducer.

For a focusing aperture, Chen et al. (1994) showed that for the mirror placed in the focal plane, the diffraction loss in the frequency domain is equal to

$$D_F(z = 2F, f) = -\{1 - \exp(jG_p)[J_0(G_p) - jJ_1(G_p)]\} \tag{4a}$$

where the pressure focal gain is

$$G_p = \frac{\pi f a^2}{c_o F} \tag{4b}$$

in which f is frequency, c_o is the speed of sound in water, a is the aperture radius, and F is the focal length. Chen et al. (1997) found that this expression has only a weak

dependency of frequency. If the argument parameter G_p is large, an asymptotic expression for Bessel functions of large arguments (Eq. 9.2.1 of Abramowitz and Stegun, 1964), can be used to approximate Eq. (4a) by

$$D_F(z = 2F, f) \approx -\{1 - \sqrt{\frac{2}{\pi G_p}} \exp\left(\frac{j\pi}{4}\right)\} = -\{1 - \frac{1}{\sqrt{\pi G_p}} - \frac{j}{\sqrt{\pi G_p}}\} \qquad (5)$$

When $G_p \geq 16$ the error of either the real or imaginary part of Eq. (5) compared to Eq. (4a) is less than 0.042. Because the terms involving the square root are small , the main contribution is from the real part of Eq. (5). Both Eq's. (4a) and (5) vary extremely slowly with frequency over a transducer bandwidth (e.g. 90% fractional bandwidth), so to a good approximation, the frequency can be set equal to transducer center frequency, $f = f_c$. Physically the result of this small loss can be interpreted in terms of ray theory as a cone of energy focused onto a plate and reflected back, almost but not quite perfectly, along the same cone to the aperture of the transducer.

To use the transfer function defined in Eq. (5) in Eq. (2), we must account for propagation delays to and from the plate and for the case where the plate is not an ideal reflector. Then we can carry out an inverse Fourier transform to obtain the time domain response. Given that a non-ideal mirror has a plane wave pressure reflection coefficient,

$$R_F = \frac{Z_2 - Z_1}{Z_2 + Z_1} \qquad (6)$$

where Z_2 is the specific acoustic impedance of the reflector and Z_1, the characteristic impedance of the fluid, then the three rightmost terms of Eq. (3) correspond to the

following inverse Fourier transform:

$$h_T(\vec{r},t) *_t s(\vec{r},t) *_t h_R(\vec{r},t) = \text{Real}\{\Im^{-1}[D_F(\vec{r},f_c)R_F \exp(-j2\pi f(2F)/c_o)]\}$$
$$= R_F\,[\sqrt{1/(\pi G_p)} - 1]\delta(t - t_{2F}) \quad (7)$$

From Eq. (7) we can see that the acoustic propagation and scattering from plate at the focus of a transducer (that is, $h_T(\vec{r},t) *_t s(\vec{r},t) *_t h_R(\vec{r},t)$) is a scaled impulse response delayed in time by $t_{2F} = 2F/c_o$. Under these conditions, the output voltage is an amplitude scaled delayed replica of the system response e_{pe},

$$v_o(t) \approx R_F\,[\sqrt{1/(\pi G_p)} - 1]e_{pe}(t - 2F/c_o) \quad (8)$$

The round trip reference signal e_{pe} can be determined from the measured output voltage signal, $v_o(t)$, and the scaling constant from Eq. (8).

B. Scattering from a point target

Often it is necessary to determine scattering from an ideal point scatterer (explained below) rather than a flat-plate. As an example, determining the spatial impulse response (h_T and h_R) experimentally requires the use of a point scatterer. Moreover, randomly positioned point scatterers form the basis of simulation models for speckle and phantom-like objects that can be created from organized patterns of point scatterers with assigned weighting (Jensen and Munk,1997). In this section, we show how the reflection from a point scatterer can be determined from a flat-plate response.

The starting point for a model of an ideal point scatterer is that of a *rigid* (incompressible) sphere with a diameter much smaller than a wavelength, density $\rho \gg \rho_o$,

and compressibility $\kappa \ll \kappa_o$, where $c = 1/\sqrt{\rho\kappa}$ and $c_o = 1/\sqrt{\rho_o\kappa_o}$. The scattering for this sphere known to be proportional to $-k^2$ (Morse and Ingard, 1986), where $k = \omega/c_o$, and a geometrical factor A. Since the inverse Fourier transform theory of $j\omega$ is $\partial/\partial t$, $-k^2$ corresponds to the transform $(1/c_o^2)\partial^2/\partial t^2$. For this type of target at the origin,

$$s(\vec{r},t) = \frac{A}{c_o^2}\frac{\partial^2}{\partial t^2} *_t \delta(t - |\vec{r}|/c_o) \tag{9a}$$

where A is a time-independent quantity that is given by (Eq.8.2.19, Morse and Ingard, 1986)

$$A = \frac{a^3}{3}(1 - \frac{3}{2}\cos\theta) \tag{9b}$$

where a is the radius of the scatterer and θ is the scattering angle. The $1/|\vec{r}|$ dependence has been absorbed into the receive factor h_R (Hunt et al. 1983). For direct backscatter $\theta = \pi$ and A has the value

$$A = \frac{5a^3}{6}. \tag{9c}$$

Real transducers have a finite aperture and collect signals over a range of angles, however, for $160 < \theta < 200$, which is appropriate for most ultrasound imaging scenarios, the variation in A over the surface of the transducer is less than 5% and the use of Eq. (9c) is appropriate. If this target is placed at the focal point, then each of the spatial impulse responses in Eq. (1) reduces to an impulse function centered on $|\vec{r}|/c_o$ (Hunt et al.,1983),

$$h_T(\vec{r},t) = h_R(\vec{r},t) = \ell\delta(t - |\vec{r}|/c_o) \tag{10a}$$

where (Arditi et al., 1981 Eq. 7)

$$\ell = F\left[1 - \left(1 - \frac{a^2}{F^2}\right)^{1/2}\right] \tag{10b}$$

Putting these results into Eq. (1) for a small spherical target at the focal point, we find

$$v_o(t) = \frac{A\ell^2}{c_o^2}\frac{\partial^2 e_{pe}(t - 2|\vec{r}|/c_o)}{\partial t^2} \tag{10c}$$

therefore, the reflected signal from a point target will have the same shape as the doubly differentiated reference waveform, $e_{pe}(t)$ with the respect to time.

Although we derived this in terms of a rigid sphere target we note that other targets smaller than a wavelength have a similar functional dependency in the backscattered direction ($\theta = \pi$) towards the transducer at distances greater than a few wavelengths (Rayleigh, 1872; Pierce, 1989). In particular, Nassiri and Hill (1986) have shown that back scatter from a disc is similar to that of a sphere, differing only in the constant A. Both the sub-wavelength sphere and disc are practical realizations of an ideal point target as viewed at moderate to large distances. Because of the practical difficulties involved in realizing a point target, it may be difficult to determine the constant A. An alternative approach to calibration described by Hunt et al. (1983) is to redefine the electromechanical response based on a point target. Their electromechanical response would be the equivalent of e_{pe} convolved with s for a point target from Eq. (1) and would include a double differentiation with time. However, if A is not known it is not possible to apply the calibration to the problem of quantitative imaging.

C. Scattering from arbitrary shaped weak scatterers: Born Approximation

In the previous two sections we showed that the electromechanical impulse response of a transducer can be measured using either a plate or a point target. Once this reference signal is known, it can be applied to simulate the backscattered field from arbitrary shaped targets through the Born approximation (Jensen,1991).

Jensen's time domain formulation of the Born approximation provides a computationally compact and useful method for simulating the back scattered field from arbitrary shaped weak scatterers for inhomogeneous medium. Equation (44) of (Jensen,1991) can be rearranged according to Eq. (1):

$$v_o(\vec{r}_5,t) = e_{pe}(t) *_t [s(\vec{r}_1) *_r \frac{\partial^2 H_{pe}(\vec{r}_1,\vec{r}_5,t)}{\partial t^2}] \tag{11}$$

in which $\vec{r}_5$ is the vector to a characteristic position of the transducer and $\vec{r}_1$ represents a vector to a point within the scatterer (Fig. 1) and, as defined by Jensen (1991),

$$H_{pe}(\vec{r}_1,\vec{r}_5,t) = h(\vec{r}_1,\vec{r}_5,t) *_t h(\vec{r}_5,\vec{r}_1,t) \tag{12}$$

is equivalent to $h_T *_t h_R$ in our Eq. (1). More explicitly, Eq. (11) is

$$\begin{aligned} v_o(\vec{r}_5,t) &= e_{pe}(t) *_t \left[\int_{V'} \left[\frac{\triangle\rho(\vec{r}_1)}{\rho_o} - \frac{2\triangle c(\vec{r}_1)}{c_o}\right] \frac{1}{c_o^2} \frac{\partial^2 H_{pe}(\vec{r}_1,\vec{r}_5,t)}{\partial t^2} d^3_{\vec{r}_1}\right] \\ &= \frac{1}{c_o^2}\frac{\partial^2 e_{pe}(t)}{\partial t^2} *_t \left[\int_{V'} \left[\frac{\triangle\rho(\vec{r}_1)}{\rho_o} - \frac{2\triangle c(\vec{r}_1)}{c_o}\right] H_{pe}(\vec{r}_1,\vec{r}_5,t) d^3_{\vec{r}_1}\right] \end{aligned} \tag{13}$$

where $\triangle\rho$ and $\triangle c$ are the perturbations in density and sound speed with respect to background and V' is the scattering region.

In the case of a point scatterer Eq. (13) reduces to:

$$v_o(\vec{r}_5,t) = \left[\frac{\triangle\rho(\vec{r}_1)}{\rho_o} - \frac{2\triangle c(\vec{r}_1)}{c_o}\right] \frac{1}{c_o^2}\frac{\partial^2 e_{pe}(t)}{\partial t^2} *_t h(\vec{r}_1,\vec{r}_5,t) *_t h(\vec{r}_5,\vec{r}_1,t) \tag{14}$$

which is consistent with Jensen's Eq. (50). Specifically in the case of a *point scatterer* placed at the focal point Eq. (14) reduces to the form of Eq. (10c). This observation reveals a potential area of confusion with respect to the results in (Jensen,1991) in which Eq. (14) is taken to be the response to a *flat-plate* at the focal plane. More correctly, as indicated by the results in the previous two sections of this paper, this flat-plate response is obtained by removing the double time derivative.

In this work the overall outcome of the Born approximation derived by Jensen (1991) is unchanged. However, we have used the twice time derivative of the plate response in our simulations. The method of finding $e_{pe}(t)$ described in Sections A and B can be applied directly to the more general case of scattering through the Born approximation as given by Eq. (13).

III. EXPERIMENTS

We carried out experiments to verify the fact that the scattered signal from a plate and a small scatterer are related by double differentiation in time. We used a spherically focused ultrasonic transducer, 3.5 MHz, 50.8 mm focal length, 12.8 mm radius (Model V380, Panameterics, Waltham, MA). This strongly focusing transducer (F number 2 and G_p=24) was placed in a water tank (0.8 m x 0.8 m x 1.5 m) that was filled with de-ionized de-gassed water at approximately 21°C. The transducer was operated in pulse-echo mode using a pulse-receiver (UA 5052, Panametrics, Waltham, MA). The pulser-receiver excited the transducer with a short excitation signal that approximated a delta function and the received echo was acquired on digital scope (LC 334a, LeCroy, Chestnut Ridge, NY) and transferred to a personal computer for later analysis. We investigated the reflections from two targets. The

first was a 12.5 mm thick flat acrylic plate acoustic mirror. The second target was from the cleaved end of an optical fiber 110 microns in diameter point scatterer.

Figure 2(a) shows the reflected pulse measured from the front surface of the acrylic plate, $v_o(t)$. This is the scaled pulse-echo impulse response, $e_{pe}(t)$, according to Eq. (7). Here G_p=24, so the diffraction correction factor is 0.885 and the reflection coefficient at the water-acrylic interface is R_F =0.348. Figure 3 compares three normalized waveforms 1) the signal measured from the plate 2) the signal measured from the optical fiber and 3) the doubly differentiated e_{pe} waveform obtained from Eq. (8) (note this equation gives a sign inversion). We see that carrying out the double-differentiation is crucial to obtaining good agreement between predictions based on the impulse response of the transducer (e_{pe}) and the received signal from a point scatterer. Without this operation neither the leading negative half-cycle nor the details of the ringdown are captured correctly. This result shows that the time-domain calibration function that is determined from a flat-plate can be used to predict the waveform from a point scatterer at the focus.

Once this reference signal is known, it can be applied to simulate the free diffraction field of the transducer or backscattering from other scattering targets. We used Eq. (1) with the point scatterer characteristic, Eq. (8), and the round trip spatial impulse response (Arditi et al.,1981) with 2 GHz sampling frequency in time, to simulate the echoes scattered from a small point-like target. To confirm our predictions, the optical fiber was mechanically scanned through the tank and echo waveforms recorded at each location. Figure 4 shows the measured and predicted contour maps of the amplitude envelope of the scattered fields for the case where the fiber was

placed in the focal plane and translated perpendicular to the acoustic beam axis. Figure 5 is a similar scan but at an axial distance of 53.8 mm (about 3 mm or 10 wavelengths behind of the focus). In both cases, there is a close agreement between the measured and predicted scattered field. The slight differences are attributable to imperfections in both the transducer as an ideal piston source, as determined by extensive hydrophone measurements, and the cleaved optical fiber as an isolated ideal point target. The source transducer was found to have a mildly distorted, asymmetric transmitted field when compared to simulations based on an ideal uniformly weighted piston source. pulse-echo simulations based on the point target waveform at the focal point gave slightly better agreement with measurements than those shown here; however, we believe this result to be a consequence of the imperfect realization of an ideal spherical scatterer by the cleaved optical fiber which had it own unique response characteristic, as shown in Fig. 3. These comparisons confirm that the plate-derived calibration waveform can be used to predict the response of a scatterer anywhere in the field of the transducer.

IV. CONCLUSION

We have shown, both theoretically and experimentally, that the pulse-echo impulse response of a spherically focused transducer can be measured using either a flat-plate or a point scatterer. The reflected waveforms in each case are not identical but rather related by an operation of double differentiation. Because of the difficulty of determining the precise geometry of practical realizations of sub-wavelength point targets and, consequently, the calibration constant A, a reflection from a flat-plate is recommended for determination of the reference pulse. For values of focal gain

greater than or equal to 16, the error in the approximation (Eq. (5)), is less than five percent.

The formulation in Eq. (1) and the relation between the flat-plate and point target echoes can be used to resolve differences among various calibration methods in the literature (Hunt et al., 1983; Carpenter and Stepanishen, 1984; Madsen et al., 1984; Jensen, 1991; Bridal et al., 1996; Chen et al.,1997) each of which can be used self-consistently but may be in conflict with other methods. For example, Hunt et al., (1983) obtained a reference waveform from a point scatterer but their formulation for the scatterer does not include the double differentiation of Eq. (10c). Their waveform is used consistently to simulate speckle as a summation of random point scatterers.

The time domain Born approximation of Jensen (1991) in Eq. (13) includes the double differentiation and shows that the echo signal from an inhomogeneous medium can be obtained by convolving the point-scattered waveform with the medium properties in agreement with Eq.'s (1) and (9a). If one wishes to use the signal measured from a flat-plate for this Born model, it is necessary to differentiate the reference signal twice with respect to time first. The wording in Jensen (1991) could be misinterpreted to mean that the flat-plate signal was already differentiated.

In summary, the commonly used reference waveform from a flat-plate target in the focal plane of a strongly focusing transducer ($G_p \geq 16$) is appropriate to determine $e_{pe}(t)$ without distortion. This reference signal is useful for transducer calibration and diffraction correction (Sigelmann and Reid, 1973; Reid, 1974; Chen et al., 1997; Machado and Foster, 1998). However, the waveform must be used with care for other scattering targets.

ACKNOWLEDGMENTS

This work was supported in part by CenSSIS, (the Center for Subsurface Sensing and Imaging Systems), under the Engineering Research Centers Program of the National Science Foundation (award number EEC-9986821). The authors are grateful for technical assistance provided by Yuan Jing in setting up the experiments.

REFERENCES

Abramowitz, M., and Stegun, I. A., *Handbook of Mathematical Functions*, Chap. 9, Dover Publications, N.Y., 1964.

Arditi, M., Foster, S. F., and Hunt, J. W., Transient fields of concave annular arrays, *Ultrasonic Imaging* 3: 37-61 (1981).

Bridal, S. L.,Wallace, K. D., Trousil, R. L., Wickline, S. A., and Miller, J. G., Frequency dependence of acoustic backscatter from 5 to 65 MHz (0.06<ka<4.0) of polystyrene beads in agarose, *J. Acoust. Soc. Am.* 100:1841-1848 (1996).

Carpenter, R. N., and Stepanishen, P. R., An improvement in the range resolution of ultrasonic pulse echo systems by deconvolution, *J. Acoust. Soc. Am.* 75:1084-1091 (1984).

Chen, X., Phillips, D.,Schwarz, K. Q., Mottley, J. G., and Parker, K. J.,The measurement of backscatter coefficient from a broadband pulse-echo system: a new formulation, *IEEE Trans. Ultrason. Ferroelectr. Freq. Control* 44:515-525 (1997).

Chen, X., Schwarz, K. Q., Parker K.J., Acoustic coupling from a focused transducer to a flat plate and back to the transducer, *J. Acoust. Soc. Am.* 95:3049-3054. (1994).

Hunt, J. W., Arditi, M., and Foster, F. S., Ultrasound transducers for pulse-echo medical imaging, *IEEE Trans Biomedical Engr* BME-30, 453-481, 1983.

Jensen, J. A., A model for the propagation and scattering of ultrasound in tissue. *J. Acoust. Soc. Am.* 89:182-190 (1991).

Jensen, J. A. and Munk, P., Computer phantoms for simulating ultrasound B-mode and cfm images, *23rd Acoustical Imaging Symposium*, Boston, Massachusetts, USA, April 13-16, 1997.

Madsen, E. L., Insana, M. F., and Zagzebski, J. A., Method of data reduction for accurate determination of acoustic backscatter coefficients, *J. Acoust. Soc. Am.* 76:913-923 (1984).

Machado, J. C. and Foster, F. S., Experimental validation of a diffraction correction model for high frequency measurement of ultrasound backscatter coefficients, 1998 *IEEE Ultrasonics Symp. Proc.* : 1869-1872.

Morse, P. M. and Ingard, K. U., *Theoretical Acoustics*, Chap. 8, Princeton University Press, Princeton, N. J., 1986.

Nassiri, D. K., and Hill, C. R. , The use of angular acoustic scattering measurements to estimate structural parameters of human and animal tissues, *J. Acoust. Soc. Am.* 79:2048:2054

(1986).

Pierce, A. D., *Acoustics*, Chap. 9, Acoustical Society of America, Woodbury, NY, 1989.

Rayleigh, J. W. S., Investigation of the disturbance produced by a spherical obstacle on the waves of sound, *Proc. London Math. Soc.*. 4:253-283 (1872).

Reid, J. M., Self-reciprocity calibration of echo-ranging transducers, *J. Acoust. Soc. Am.* 55: 862-868 (1974).

Rhyne, T. L., Radiation coupling of a disk to a plane and back or a disk to disk: An exact solution, *J. Acoust. Soc. Am.* 61:318-324. (1977).

Rogers, P. H., and Van Buren, A. L., An exact expression for the Lommel diffraction correction integral, *J. Acoust. Soc. Am.* 55:724-728 (1974).

Seki, H.,Granato, A., and Truell, R., Diffraction effects in the ultrasonic field of a piston source and their importance in the accurate measurement of attenuation, *J. Acoust. Soc. Am.* 28:230-238 (1956).

Sigelmann, R. A., and Reid, J. M., Analysis and measurement of ultrasonic backscattering from an ensemble of scatterers excited by sine-wave bursts, *J. Acoust. Soc. Am.* 53:1351-1355 (1973).

Thijssen, J. M., Spectroscopy and image texture analysis, *Ultrasound in Medicine and Biology*, Vol 26,1, (2000), S41-S44

FIGURE CAPTIONS

1. Schematic showing the transducer/scatterer arrangement and the theoretical and experimental coordinate systems.

2. (a) Reference pulse-echo from a large thick acrylic plate placed in the geometric focal plane of a 3.5 MHz spherically focused transducer. (b) Amplitude spectrum of pulse-echo.

3. Comparison of the flat-plate pulse-echo (Fig. 2(a), normalized and filtered), differentiated flat-plate pulse-echo (Fig. 2(a), normalized and doubly differentiated with respect to time) and a pulse-echo from the tip of an optical fiber placed at the geometric spherical focal point of a 3.5 MHz transducer.

4. (a) Amplitude envelope of the pulse-echo field of 3.5 MHz transducer as measured by scanning an optical probe laterally at an axial distance equal to the focal length. (b) Amplitude envelope of the simulated pulse-echo field using Eq. (10c) and differentiated signal from Fig. 3.

4. (a) Amplitude envelope of the pulse-echo field of 3.5 MHz transducer as measured by scanning an optical probe laterally at an axial distance z=53.8 mm. (b) Amplitude envelope of the simulated pulse-echo field using Eq. (10c) and differentiated signal from Fig. 3.

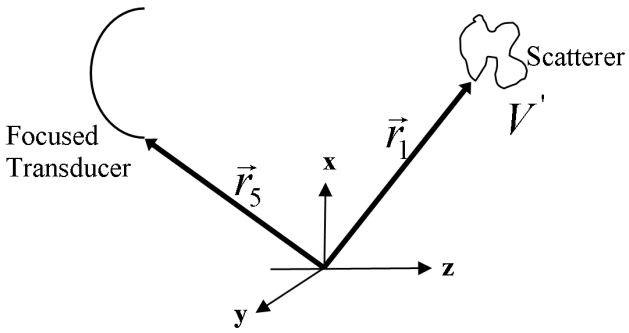

FIG. 1.

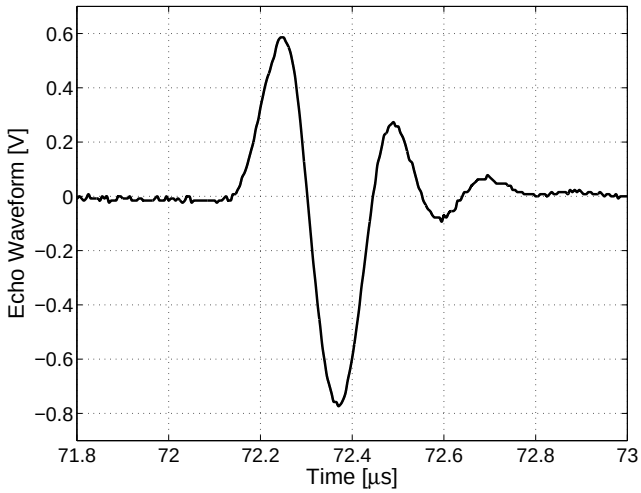
Echo Waveform [V]
0.6
0.4
0.2
0
−0.2
−0.4
−0.6
−0.8
71.8
72
72.2
72.4
72.6
72.8
73
Time [µs]

(a)

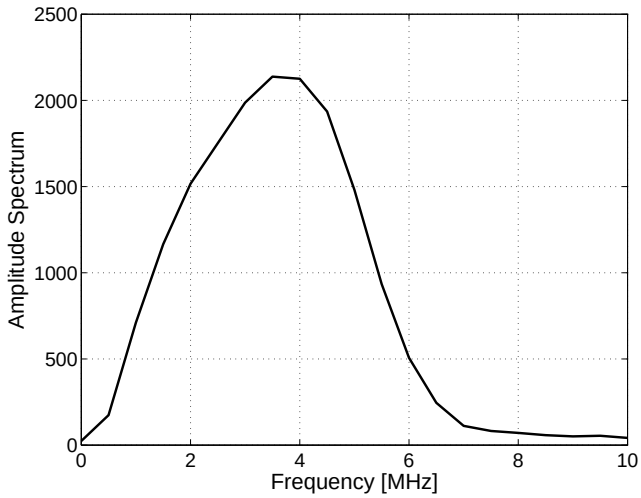
Amplitude Spectrum
2500
2000
1500
1000
500
0
0
2
4
6
8
10
Frequency [MHz]

(b)

FIG. 2.

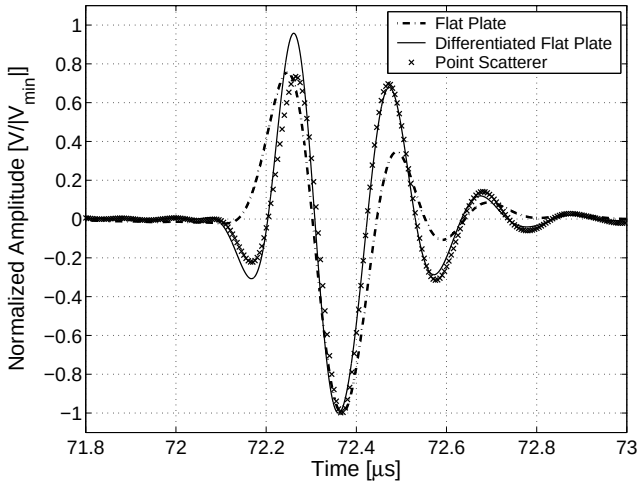
Flat Plate
Differentiated Flat Plate
Point Scatterer
Normalized Amplitude [V/|V_min|]
Time [μs]
1
0.8
0.6
0.4
0.2
0
−0.2
−0.4
−0.6
−0.8
−1
71.8
72
72.2
72.4
72.6
72.8
73

FIG. 3.

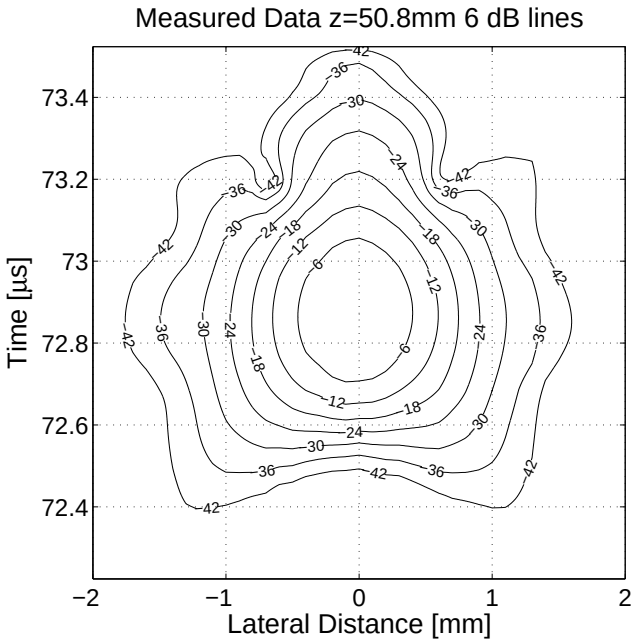
Measured Data z=50.8mm 6 dB lines
Time [µs]
Lateral Distance [mm]
73.4
73.2
73
72.8
72.6
72.4
−2
−1
0
1
2

(a)

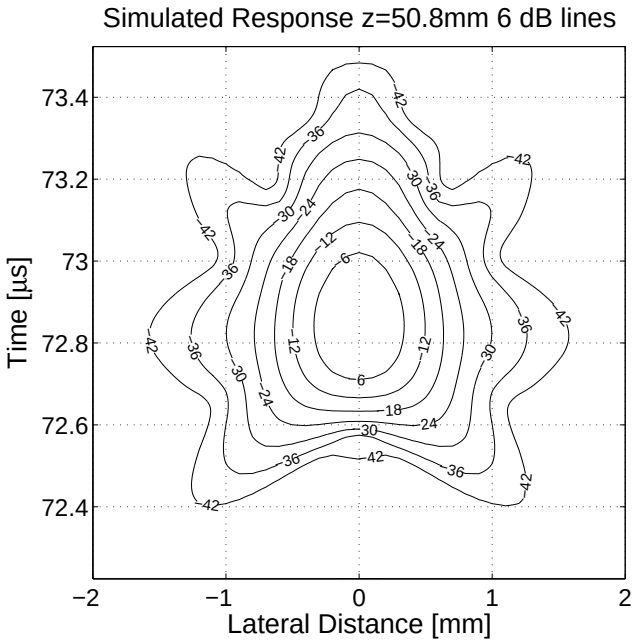
Simulated Response z=50.8mm 6 dB lines
Time [µs]
Lateral Distance [mm]
73.4
73.2
73
72.8
72.6
72.4
−2
−1
0
1
2

(b)

FIG. 4.

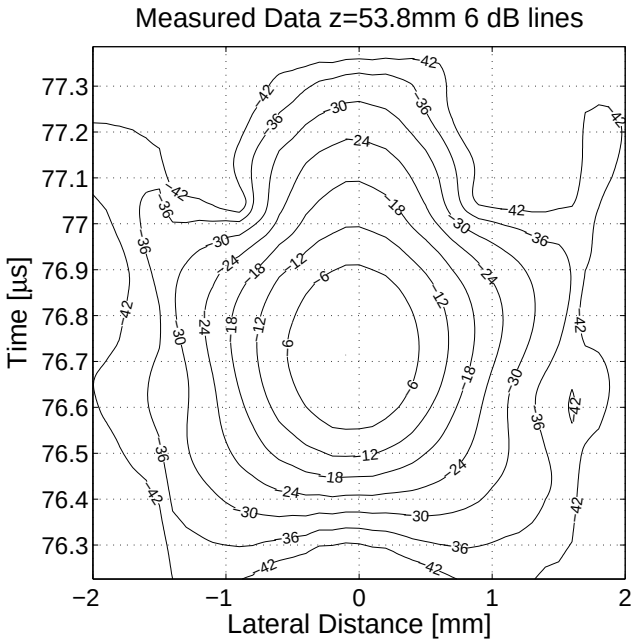
Measured Data z=53.8mm 6 dB lines
Time [µs]
Lateral Distance [mm]
77.3
77.2
77.1
77
76.9
76.8
76.7
76.6
76.5
76.4
76.3
−2
−1
0
1
2

(a)

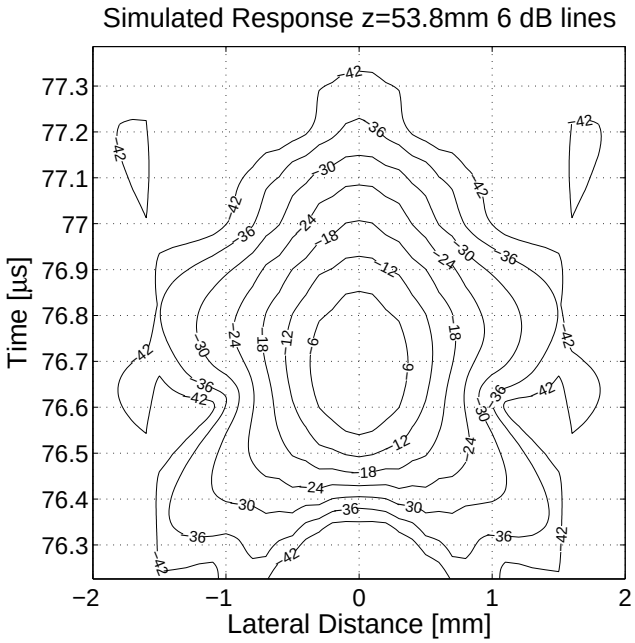
Simulated Response z=53.8mm 6 dB lines
Time [µs]
Lateral Distance [mm]
77.3
77.2
77.1
77
76.9
76.8
76.7
76.6
76.5
76.4
76.3
−2
−1
0
1
2

(b)

FIG. 5.